

Preferential Partitioning of Per- and Polyfluoroalkyl Substances (PFAS) and Dissolved Organic Matter in Freshwater Surface Microlayer and Natural Foam

Summer L. Sherman-Bertinetti, Edward G. Kostelnik, Kaitlyn J. Gruber, Sarah Balgooyen, and Christina K. Remucal*



Cite This: <https://doi.org/10.1021/acs.est.4c02285>



Read Online

ACCESS |



Metrics & More



Article Recommendations



Supporting Information

ABSTRACT: Per- and polyfluoroalkyl substances (PFAS) are surfactants that can accumulate in the surface microlayer (SML) and in natural foams, with potential elevated exposure for organisms at the water surface. However, the impact of water chemistry on PFAS accumulation in these matrices in freshwater systems is unknown. We quantified 36 PFAS in water, the SML, and natural foams from 43 rivers and lakes in Wisconsin, USA, alongside measurements of pH, cations, and dissolved organic carbon (DOC). PFAS partition to foams with concentration ranging 2300–328,200 ng/L in waters with 6–139 ng/L PFAS (sum of 36 analytes), corresponding to sodium-normalized enrichment factors ranging <50 to >7000. Similar enrichment is observed for DOC (~70). PFAS partitioning to foams increases with increasing chain length and is positively correlated with [DOC]. Modest SML enrichment is observed for PFOS (1.4) and FOSA (2.4), while negligible enrichment is observed for other PFAS and DOC due to low specific surface area and turbulent conditions that inhibit surfactant accumulation. However, DOC composition in the SML is distinct from bulk water, as assessed using high-resolution mass spectrometry. This study demonstrates that natural foams in unimpacted and impacted waters can have elevated PFAS concentrations, whereas SML accumulation in surface waters is limited.

KEYWORDS: PFAS, surface microlayer, natural foam, freshwater, DOM

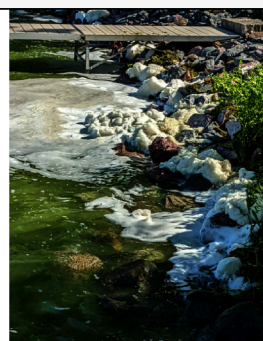
Average PFAS and DOC Enrichment

Natural Foams
80 (PFOA) – 4,000 (PFDA)
70 (DOC)

>>>

Lake Surface Microlayer
1 (PFOA) – 2.4 (FOSA)
1 (DOC)

= f(PFAS structure, water chemistry)



INTRODUCTION

Per- and polyfluoroalkyl substances (PFAS) are a group of >9000 synthetic chemicals that have been used in products such as nonstick cookware,¹ water-repellant textiles,^{2–4} and aqueous film forming foams (AFFF)^{5–9} since the 1940s.¹⁰ Some PFAS are highly persistent in the environment,^{11–13} can bioaccumulate,^{14–19} and have adverse health effects in humans and wildlife.^{20–24} PFAS have been detected globally, including in rainwater,^{25–27} in surface water, sediment, and biota of the Laurentian Great Lakes,^{15,16,18,28–30} and in remote regions, such as the Arctic Ocean, ice caps, and glaciers.^{31–33}

PFAS are amphiphilic due to their hydrophobic fluorinated carbon chain and hydrophilic headgroup. The amphiphilic nature of PFAS makes these compounds excellent surfactants that lower the surface tension of water,^{34–37} resulting in preferential partitioning to the air–water interface in which the water-soluble group is submerged in water and the hydrophobic tail is adsorbed at the air–water interface.³⁶ PFAS partitioning to the air–water interface in surface waters can impact sampling,^{35,38} aerosol formation,^{36,39,40} and exposure to organisms that spend time at the surface (e.g., birds, aquatic

mammals).³⁵ This behavior also influences PFAS transport in the subsurface^{34,41–48} and removal by carbon-based sorbents.^{49–51}

Partitioning at the air–water interface can potentially result in elevated PFAS concentrations in the surface microlayer (SML), which is the top 1–1000 μm of water column.^{52–61} Laboratory studies using fresh water^{40,59} and saline water^{39,59,61} demonstrate that PFAS may be enriched in the SML at factors of <1 to >100. Dissolved organic matter (DOM) and individual biomolecules, which also display surfactant-like behavior, can similarly preferentially partition to the SML.^{53,54,56–59} Thus, DOM behavior may provide insight into PFAS partitioning in surface waters.

Received: March 4, 2024

Revised: July 2, 2024

Accepted: July 3, 2024

Despite the potential importance of SML partitioning in PFAS fate in aquatic systems, available field data on SML enrichment are limited to three studies in marine systems^{35,38,60} and a single study on an AFFF-impacted freshwater lake.⁶ In marine systems, enrichment factors range from 1 to 109 for PFOA and from 1.2 to 6.5 for PFOA, suggesting sulfonates are more likely to partition to the SML.^{35,38,60} Lower enrichment factors of 4.4–12 for PFOS and 0.9–1.8 for PFOA were observed in a freshwater lake,⁶ in agreement with observations that PFAS partitioning is influenced by ionic strength.^{36,37,45,47,59,62,63} Additional factors may also influence PFAS partitioning. For example, DOM may either decrease or increase PFAS partitioning to the SML (i.e., via competition or via sorption of PFAS to DOM at the air–water interface).^{36,37,39,59} PFAS concentrations could also influence partitioning.³⁷ Thus, further investigation of PFAS partitioning to the SML in freshwater systems that range widely in both PFAS and dissolved organic carbon (DOC) concentrations is needed.

PFAS enrichment at the SML has implications for foams that form on surface waters. Foams are often assumed to be anthropogenic in origin, and their visibility draws public attention, in contrast with hidden chemical pollution (e.g., metals, pesticides).^{64–66} However, most foams are naturally occurring.^{64–66} Foam formation requires the presence of a surface-active material and a way to introduce air bubbles, such as hydraulic structures (e.g., dams/spillways), high flow events, or windy conditions.^{64,65} Natural surfactants may be derived from algae and plants (e.g., DOM), while anthropogenic foams are historically linked to phosphates and detergents.^{64,66} Natural foams may serve as a food source or habitat, while anthropogenic foams can be toxic to aquatic organisms or influence chemical transport.^{64,67}

High PFAS concentrations (~10,000–100,000 ng/L) in foams have prompted Wisconsin and Michigan to issue warnings about contact with foams in freshwaters,^{68,69} as well as concerns about contact with sea foam in the Netherlands.^{70,71} These concentrations correspond to enrichment factors of 10 to >2000 compared to bulk water,⁷ although these values may overestimate the extent of enrichment because they are based on condensed foam (e.g., 2 L of foam condensed to <80 mL for analysis). The presence of foams in freshwaters could potentially be used to identify water bodies with elevated PFAS concentrations, while intentional production of foams (i.e., foam fractionation) has been proposed for PFAS remediation.^{72–77} Laboratory foam fractionation studies indicate that PFAS partitioning increases with increasing [PFAS],⁷³ decreasing pH,⁷³ and increasing ionic strength,^{73,75} but these factors have not been evaluated in natural systems.

There are limited data on PFAS and DOC partitioning in the surface microlayer and natural foam in freshwater systems as well as on how water chemistry impacts this behavior. This study therefore aims to quantify PFAS and DOC in foam, the surface microlayer, and bulk water in surface waters that range widely in [PFAS] and [DOC] and to relate field-derived enrichment factors to water chemistry, including pH, [DOC], and Σ [cations]. We also use bulk- and molecular-level measurements to assess how DOM composition changes during partitioning to both media and relate this behavior to trends observed in PFAS as a function of its structure. This study provides insight into the prevalence of PFAS in foams and the SML in surface waters as well as the underlying factors that influence PFAS partitioning in these media.

MATERIALS AND METHODS

Materials. Chemicals used for sample preparation and liquid chromatography-tandem mass spectrometry (LC-MS/MS) analysis, including native PFAS standards (36), mass-labeled surrogates (24), and nonextracted internal standards (2), are described in the [Supporting Information, Section S1](#). Ultrapure water was supplied by a MilliporeSigma Milli-Q water system (18.2 M Ω ·cm).

Field Sample Collection. Natural foam, bulk water, and surface microlayer samples were obtained in 2020–2023 in Wisconsin, USA ([Table S2](#)). Fourteen paired foam and bulk water samples were collected from eight lakes, one river, and one creek during foaming events, which typically occurred on windy days. Additional foam samples without paired water samples were obtained at seven sites. Foam sites included sites directly impacted by AFFF (e.g., Lakes Monona and Waubesa, the bay of Green Bay) and sites with lower PFAS concentrations (e.g., Lake Mendota, Rock Lake, and Lake Noquebay) to investigate the impact of [PFAS] on foam accumulation.

Paired surface microlayer and bulk water samples were collected from 28 lakes, rivers, and creeks under baseflow conditions including six foam sites. Samples were collected downstream of airports (e.g., Starkweather Creek, Oak Creek, and Kinnikinnic River) and from sites with lower PFAS concentrations (e.g., Lake Mendota and Milwaukee River). Replicate SML samples were obtained at six sites and analyzed for reproducibility ([Section S3](#)).

Foam samples for PFAS were collected as described previously.⁷⁸ Briefly, foam was scooped by a gloved hand into Ziploc bags and allowed to condense into a liquid at 4 °C. The liquid was diluted with methanol to ~80:20 MeOH:foam (v/v), homogenized within the bag to allow for desorption of longer chain PFAS from bag walls, and transferred into 250 mL polypropylene bottles for storage.

Bulk water samples for PFAS analysis were collected by submerging a closed 250 mL polypropylene bottle 10–25 cm below the water surface, opening the bottle to collect water, and closing the bottle before lifting the sample.

Surface microlayer samples for PFAS were collected using the glass plate method.^{6,79} Briefly, a 2.36 mm thick glass plate (25.4 cm \times 30.5 cm) was first rinsed with the bulk water sample. The rinsed plate was then held perpendicular to the water with a gloved hand and slowly dipped into and out of the water column. The water collected onto the glass plate was drained into a 250 mL polypropylene bottle. The process was repeated until the bottle was full. Samples were frozen at –18 °C and thawed prior to analysis.

Water and SML samples for background water chemistry were syringe filtered (0.45 μ m, nylon) on-site and stored in 40 mL amber glass vials for analysis of pH, dissolved organic carbon concentration ([DOC]), UV–visible (UV–vis) spectra, and fluorescence spectra. Parallel samples were filtered and stored in 15 mL polypropylene Falcon tubes for cation analysis. Additional foam samples were collected in Ziploc bags for background water chemistry and allowed to condense into a liquid at 4 °C. Collapsed samples were diluted with ultrapure water (~1:20 foam:water), filtered (0.45 μ m, nylon), and stored in 40 mL amber glass vials (pH, [DOC], UV–vis, and fluorescence) or 15 mL polypropylene Falcon tubes (cations).

Five additional paired surface microlayer and bulk water samples were collected for Fourier transform-ion cyclotron resonance mass spectrometry (FT-ICR MS) analysis of the

DOM composition (Table S2). Samples were filtered (0.45 μm , glass fiber) within 48 h and stored in amber glass jars (baked at 450 $^{\circ}\text{C}$ for 8 h) at 4 $^{\circ}\text{C}$ in the dark.

PFAS Quantification. Water, foam, and SML samples were analyzed for 13 perfluoroalkyl carboxylic acids (PFCAs; C_4 – C_{14} , C_{16} , C_{18}), 8 perfluoroalkyl sulfonic acids (PFSAs; C_4 – C_{10} , C_{12}), 4 fluorotelomer sulfonates (FTSs; C_4 , C_6 , C_8 , C_{10}), 3 perfluorooctane sulfonamides, 2 perfluorooctane sulfonamidoacetic acids, 2 perfluorooctane sulfonamide ethanols, and 4 ether-containing fluorosubstances. Bulk water and SML samples were extracted following a modified version of U.S. Environmental Protection Agency (EPA) method 1633 (Section S1.2.2)⁸⁰ and analyzed by LC-MS/MS. Diluted foam samples were filtered (0.2 μm , nylon) and analyzed directly by LC-MS/MS.⁷ Instrumental details are described in Section S1. Due to low suspended solid concentrations (Table S16), PFAS measurements represent aqueous concentrations. QA/QC details are provided in Section S3. Unless otherwise noted, reported PFAS concentrations are summed peak areas for linear and branched isomers. Linear isomer concentrations are reported for a subset of PFAS (Table S3).

Background Chemistry. Background chemistry parameters were measured in filtered water and SML samples as well as in foam diluted with ultrapure water. [DOC] was measured with a Total Organic Carbon Analyzer. Cations were measured by inductively coupled plasma-optical emission spectroscopy. UV-vis and fluorescence spectra were collected using a Shimadzu spectrophotometer and Horiba Aqualog, respectively. Details are provided in Section S1.4.

FT-ICR MS Analysis. Water and SML samples (500 mL) were extracted via solid phase extraction (SPE) as described previously^{81–83} and analyzed by FT-ICR MS (Solarix XR 12T) with negative electrospray ionization. Ions with $S/N > 3$ and intensity $> 1,000,000$ were exported. Exported ions were converted to neutral masses, linearly calibrated using common DOM formulas, and matched to potential chemical formulas ($\text{C}_{0-80}\text{H}_{0-1}\text{O}_{0-140}\text{N}_{0-2}\text{S}_{0-1}$) in R as described previously.^{83–88} Weighted averages of elemental ratios ($\text{H}:\text{C}_w$ and $\text{O}:\text{C}_w$), double bond equivalents (DBE_w), and molecular weight (MW_w) were calculated from identified formulas to compare DOM compositional differences in the water column and surface microlayer (Section S1.4.3).

Enrichment Factor Calculations. Enrichment factors ($\text{EF}_{\text{foam,norm}}$) were calculated by normalizing to sodium concentrations in each matrix:

$$\text{EF}_{\text{foam,norm}} = \frac{[\text{PFAS}]_{\text{foam}}/[\text{Na}^+]_{\text{foam}}}{[\text{PFAS}]_{\text{water}}/[\text{Na}^+]_{\text{water}}} \quad (1)$$

Sodium normalization is used in marine systems when investigating SML enrichment⁵⁶ and, importantly, corrects for the fact that this comparison relates a condensed foam sample (e.g., a 3.8 L foam sample condenses to 35–80 mL) to a bulk water sample. $\text{EF}_{\text{foam,norm}}$ was calculated only for compounds that were present in both foam and bulk water samples and was therefore limited to three PFCAs (PFOA, PFNA, and PFDA), PFOS, and FOSA. $\text{EF}_{\text{SML,norm}}$ was calculated similarly. Non-normalized enrichment factors (EF_{foam} or EF_{SML}) that relate $[\text{PFAS}]_{\text{foam}}$ directly to $[\text{PFAS}]_{\text{water}}$ or $[\text{PFAS}]_{\text{SML}}$ directly to $[\text{PFAS}]_{\text{water}}$ respectively, were also included to enable comparison with previous studies^{7,59} and to calculate values for 2020 and 2021 samples that did not have sodium measurements.

Linear Regression Analysis. Linear regression analysis was performed on normally distributed data to identify correlations between PFAS and DOC enrichment and water chemistry parameters. A Shapiro–Wilks test was applied to determine if each data set was normally distributed; data were transformed if the original data set was significantly different than normal ($p \leq 0.05$, Section S1.4.7).

RESULTS AND DISCUSSION

PFAS Partitioning in Foam. Foam samples were collected in lakes and rivers that range widely in PFAS concentrations (Table S2). Sites with known PFAS sources include water bodies that are impacted by historical AFFF use at the Dane County Regional Airport (e.g., Lakes Monona, Waubesa, and Kegonsa),^{89–91} as well as sites near an AFFF testing facility in Marinette, Wisconsin (e.g., Green Bay shore).^{92,93} Many of the other sites, including Lakes Mendota and Wingra, are not currently associated with known PFAS sources.

Elevated PFAS concentrations are observed in naturally formed foams in both highly impacted and less impacted waters. Targeted PFAS concentrations in condensed foam samples range from 2320 ng/L in Pheasant Branch Creek to 328,190 ng/L in Lake Monona (sum of 36 analytes; Figure 1a and Figures S7

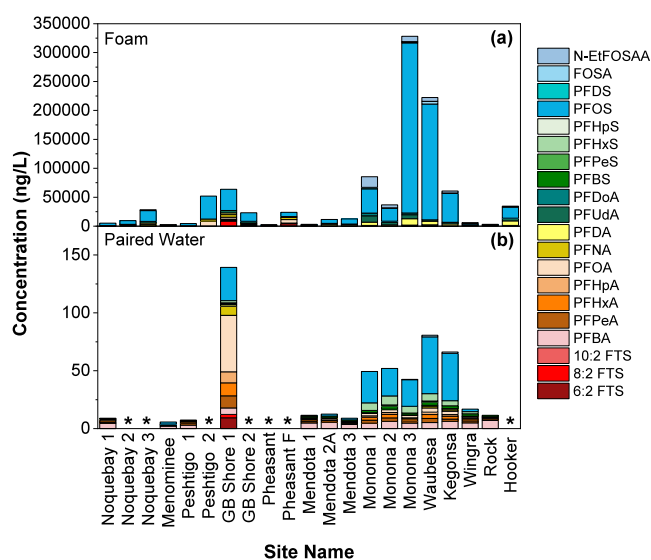


Figure 1. PFAS concentrations (ng/L) in (a) collapsed foam and (b) paired bulk water samples. Samples are grouped by the geographical location (Figures S2–S4). Asterisks (*) denote sites where paired bulk water samples were not collected. The same data are plotted on a log scale in Figure S7.

and S8, Table S21), with mean and median concentrations of 46,470 and 17,770 ng/L, respectively. Of the 36 targeted PFAS compounds across eight different classes, only 15 analytes comprising five classes are detected in at least one foam sample (Table S24). Note that the limits of detection are higher in foam because foam samples are not concentrated by SPE (Table S17). The dominant PFAS classes in foams are PFSAs ($56 \pm 19\%$ of targeted PFAS by concentration on average) and PFCAs ($38 \pm 19\%$). PFAS in foams are dominated by long-chain ($\text{C}_{\geq 8}$) compounds, which make up 100% of PFSAs and $98 \pm 4\%$ of PFCAs by concentration.

PFAS concentrations in parallel bulk water samples are orders of magnitude lower than condensed foam samples and range from 6 ng/L in the Menominee River to 139 ng/L in Green Bay

Shore 1 (mean = 35 ng/L; median = 13 ng/L; Figure 1b and Figure S7, Table S22). The 16 analytes detected in paired water samples tend to be shorter chain PFAS (Table S25). Analytes present in foam and absent in paired water samples include *N*-EtFOSAA, 10:2 FTS, PFDoA, and PFDS. Analytes present in paired water samples yet absent in foam are PFBA, PFBS, PFPeS, PFHxS, and PFHpS. This results in higher abundances of short chain PFAS in water samples compared to foams (i.e., only $60 \pm 25\%$ of PFSA and $21 \pm 14\%$ of PFCAs in water are $C_{\geq 8}$ compounds by concentration). Furthermore, water concentrations are dominated by PFCAs ($63 \pm 27\%$) rather than PFSA (36 \pm 27%), which is opposite to the distribution in foams. Water samples also have lower abundances of L-PFOS compared to foams in Dane County Lakes (Figure S11), which is similar to observations in an AFFF-impacted lake.⁷

Enrichment factors demonstrate that PFAS preferentially partition into natural foams. Mean $EF_{\text{foam, norm}}$ values are 81 for PFOA ($n = 2$; range = 47–115), 644 for PFNA ($n = 5$; 51–1035), 4012 for PFDA ($n = 2$; 530–7493), 1563 for total PFOS ($n = 10$; 195–4439), 1879 for L-PFOS ($n = 6$; 267–5196), and 1431 for FOSA ($n = 2$; 87–2776; Figure 2a, Table S31). Mean EF_{foam} values are larger than normalized values at 107 for PFOA ($n = 3$; range = 72–131), 1265 for PFNA ($n = 6$; 349–3040), 4967 for PFDA ($n = 3$; 2134–9234), 3514 for total PFOS ($n = 12$; 958–10,596), 4411 for L-PFOS ($n = 6$; 1337–14,990), and 2020 for FOSA ($n = 2$; 564–3476; Table S32). Additional EF_{foam} values in Green Bay Shore 1, which is impacted by

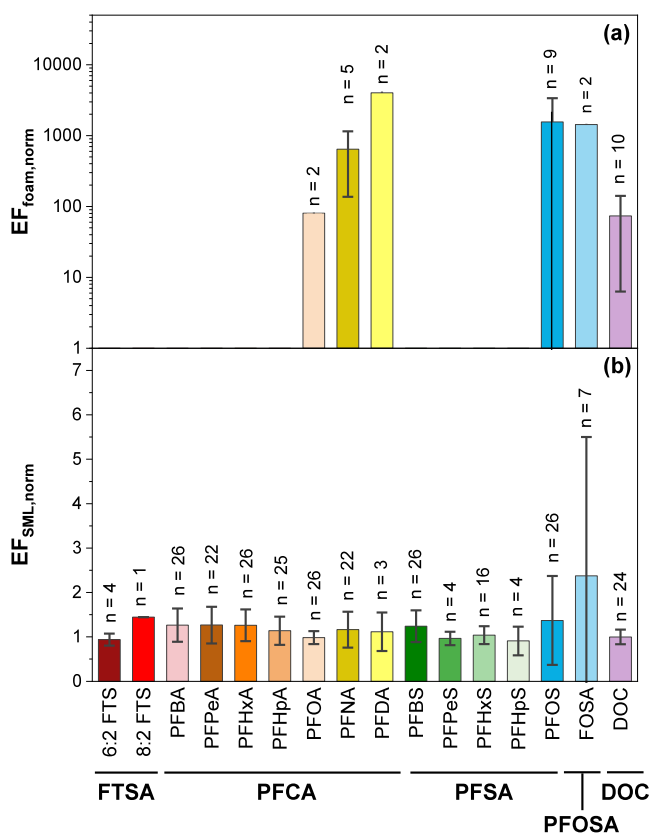


Figure 2. Average sodium-normalized enrichment factors for (a) foam and (b) the surface microlayer (SML) for PFAS and DOC. The number of paired water samples is indicated. Error bars correspond to the standard deviation of values for compounds with ≥ 3 pairs. Note that the $EF_{\text{foam, norm}}$ values are on a log scale. Nonnormalized enrichment factors are presented in Figure S12.

AFFF,⁹³ are 2895 for 8:2 FTS, 62 for PFPeA, 80 for PFHxA, 56 for PFHpA, and 4415 for PFUDA. EF_{foam} values for PFHxA, PFOA, and PFOS are similar to nonnormalized EF_{foam} values of 10 (PFHxA), 29–92 (PFOA), and 77–4371 (L-PFOS) in an AFFF-impacted lake.⁷ EF_{foam} values for the remaining compounds have not been previously reported. Note that these values consider dissolved PFAS concentrations; future work on PFAS partitioning to particles within foams is warranted.⁹⁴

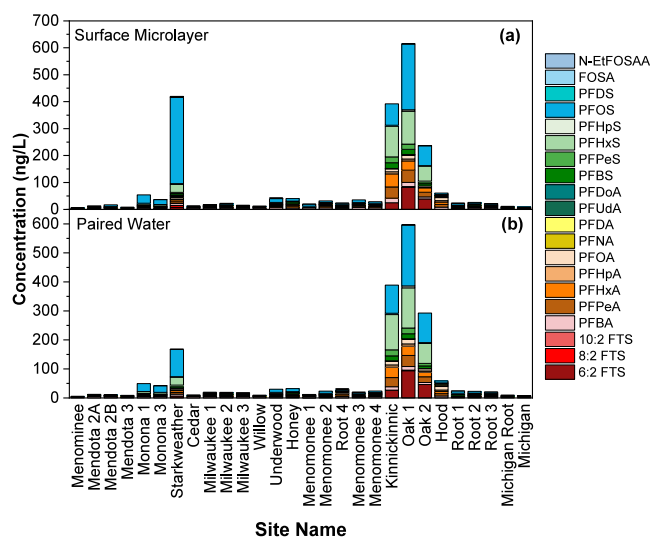


Figure 3. PFAS concentrations (ng/L) in the (a) surface microlayer and (b) paired bulk water. Samples are grouped by geographical location (Figures S2–S4). Note that the samples Menominee–Monona 3 were collected on windy days (i.e., during foaming events; Table S2). The same data is plotted on a log scale in Figure S9.

Importantly, the measured $EF_{\text{foam, norm}}$ values demonstrate that molecular structure influences PFAS accumulation in foam. $EF_{\text{foam, norm}}$ increases with increasing PFCA chain length, demonstrating that longer chain species of the same class undergo preferential partitioning to natural foams. This result agrees with a previous observation in freshwater foam for two PFSA (i.e., PFHxS and PFOS) and two PFCAs (i.e., PFHxA and PFOA).⁷ In addition, $EF_{\text{foam, norm}}$ for PFOS (i.e., a C_8 PFSA) is 2.4 times greater than that for PFNA (i.e., a C_9 PFCA), which demonstrates that PFSA of the same fluorinated chain length preferentially partition to foams compared to PFCA analogues. FOSA (i.e., a C_8 PFOSA), which is a precursor to PFOS, has an $EF_{\text{foam, norm}}$ value that is similar to PFOS. Although we are only able to differentiate between linear and branched isomers for PFOS in these samples, the preferential partitioning of L-PFOS to foams agrees with similar trends for PFOS and PFHxS in a previous study.⁷

The trends in the partitioning of PFAS to natural foams are consistent with PFAS partitioning in other media. Long-chain PFAS preferentially partition to sediment^{95–99} and biota.^{5,97–100} PFSA have larger bioaccumulation factors than PFCAs of the same chain length and are therefore more likely to partition out of the water into various forms of media.^{101,102} Similarly, foam fractionation is more efficient at removing longer chain PFAS.^{72,75,77,103}

Water chemistry influences PFOS partitioning to natural foams. This analysis considers $EF_{\text{foam, PFOS}}$ values because this data set has the largest number of paired water chemistry

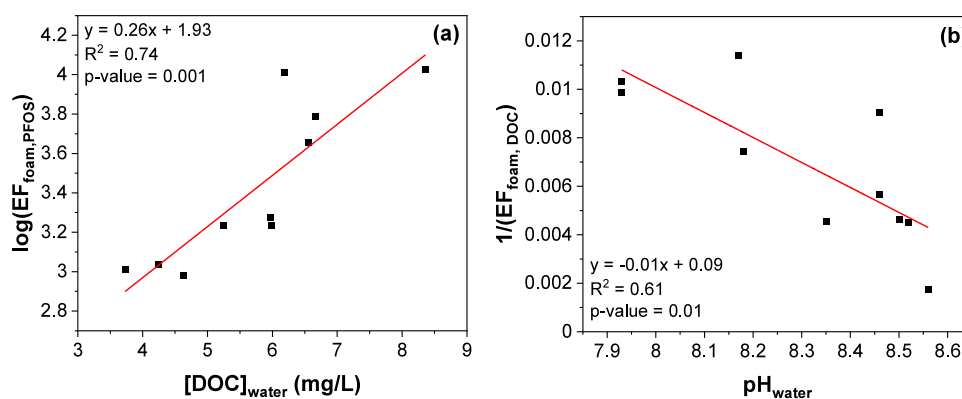


Figure 4. Linear regressions for (a) $\log(EF_{\text{foam,PFOS}})$ versus $[DOC]_{\text{water}}$ and (b) $1/(EF_{\text{foam,DOC}})$ versus pH_{water} .

measurements; trends are similar when $EF_{\text{foam, norm}}$ values are used. There is a statistically significant positive trend between $EF_{\text{foam,PFOS}}$ and $[DOC]_{\text{water}}$ ($p = 0.001$, Figure 4a), as well as weaker positive trends with $[PFOS]_{\text{water}}$ and pH_{water} (Figure S13). The trends in PFOS partitioning agree with observations of increased PFAS partitioning with increasing $[PFAS]_{\text{water}}$ ⁷³ but disagree with an observation of increased partitioning under acidic conditions during foam fractionation.⁷³ Interestingly, there is no correlation between $EF_{\text{foam,PFOS}}$ and the sum of $[cations]_{\text{water}}$, which is a proxy for ionic strength. PFAS partitioning during foam fractionation consistently increases with increasing ionic strength^{73,75}; this trend has been attributed to increased solution viscosity and decreased critical micelle concentration, which provide a more stable foam.⁷⁵ However, these samples were collected in freshwater, and there is a small range in cation concentrations (i.e., a factor of 3). This is the first comparison of EF_{foam} with water chemistry in natural systems and the first observation of a relationship between $[DOC]_{\text{water}}$ and PFOS enrichment to foams. DOM has a surfactant-like nature and lowers surface tension at the air–water interface,³⁷ which likely contributes to enhanced foam formation and results in increased PFOS accumulation in foam because $[DOC]_{\text{water}}$ is many orders of magnitude higher in concentration (i.e., mg/L vs ng/L).

DOM Partitioning in Foam. The partitioning of dissolved organic matter to natural foams is assessed using both concentration (i.e., $[DOC]$) and composition measurements (i.e., optical properties). As observed for PFAS, $[DOC]$ is orders of magnitude higher in condensed foam (average = 1168 ± 934 mg-C/L) compared to paired bulk water samples (average = 5.8 ± 1.4 mg-C/L, Tables S5 and S6). These concentrations correspond to an average $EF_{\text{foam, norm}}$ value of 74 for DOC (Figure 2a, Table S31), which is similar to the value for PFOA. Note that targeted PFAS only account for $(1.3 \times 10^{-4})\%$ of $[DOC]_{\text{water}}$ and $(1.1 \times 10^{-3})\%$ of $[DOC]_{\text{foam}}$. The minor role of PFAS within DOC agrees with previous assessments that natural surfactants derived from algae and plants (i.e., DOM) play a key role in foam formation.^{64,66}

Differences in UV–vis and fluorescence spectroscopy parameters further demonstrate that there is preferential partitioning of DOM to foam. $E_2:E_3$ (i.e., absorbance at 250 nm divided by absorbance at 365 nm) is inversely related to direct measurements of molecular weight.^{86,104} $E_2:E_3$ is much lower in foam (average = 3.9 ± 0.4) compared to water (8.2 ± 1.7 , Tables S5 and S6), demonstrating that DOM in foam is higher in apparent molecular weight. This trend is consistent with the preferential partitioning of longer chain PFCAs (Figure

2a). Specific UV absorbance at 254 nm ($SUVA_{254}$) is related to aromaticity of DOM^{104,105} and is lower in foam (1.8 ± 0.4 L $\text{mg}^{-1} \text{C}^{-1} \text{m}^{-1}$) compared to water (0.8 ± 0.3 L $\text{mg}^{-1} \text{C}^{-1} \text{m}^{-1}$, Tables S5 and S6), indicating that aliphatic DOM preferentially partitions to foam. Indices derived from fluorescence spectra further suggest that DOM in natural foam is more terrestrial (smaller fluorescence index),^{106–109} more soil-based (smaller biological index),¹⁰⁶ includes less fresh DOM (smaller freshness index),¹⁰⁶ and is less humic (smaller humification index)^{110,111} than underlying water. These differences in optical properties demonstrate that a subset of molecules within the complex DOM pool preferentially partition to natural foams.

Water chemistry influences the partitioning of DOC to foam. There is a statistically significant positive trend between $EF_{\text{foam,DOC}}$ and pH_{water} ($p = 0.01$, Figure 4b), which is the same trend as the weaker correlation between $EF_{\text{foam,PFOS}}$ and pH_{water} . As observed for PFOS, $EF_{\text{foam,DOC}}$ is positively correlated with $[DOC]_{\text{water}}$, although the trend is not significant ($p = 0.11$, Figure S14). Interestingly, $EF_{\text{foam,DOC}}$ has a weak positive correlation with $\sum [cations]_{\text{water}}$ ($p = 0.23$). Although this trend is not significant, it aligns with observations of ionic strength impacts on PFAS partitioning during foam fractionation.^{73,75}

PFAS Partitioning to the SML. There is limited enrichment of PFAS to the surface microlayer compared to that of bulk water in lakes and rivers. Summed PFAS concentrations in the SML range from 6.6 to 615 ng/L (average = 80 ± 149 ng/L; median = 23 ng/L). Elevated concentrations are observed in Oak Creek and Kinnickinnic River, which drain the Milwaukee Mitchell International Airport,^{112,113} and in Starkweather Creek and Lake Monona, which are downstream of the Dane County Regional Airport.^{89–91} Lower PFAS SML concentrations are observed in the other sites, which are not currently associated with known PFAS sources. Only 18 analytes encompassing four classes are detected in SML samples (Figure 3a and Figures S9a and S10a, Tables S23 and S26). PFAS in the SML are $54 \pm 19\%$ PFCAs and $45 \pm 16\%$ PFASAs by concentration, with detections of fluorotelomer sulfonates in AFFF-impacted sites.

PFAS concentrations in paired bulk water samples range from 5.6 to 597 ng/L (average = 70 ± 136 ng/L; median = 22 ng/L; Figure 3b and Figures S9b and S10b, Tables S22 and S25), with higher concentrations downstream of airports. Sixteen analytes are detected in bulk water; these analytes are the same as those identified in SML samples with the exception of two compounds (i.e., PFDoA and PFDS) that are only identified in Starkweather Creek and Underwood Creek SML samples. Bulk water samples

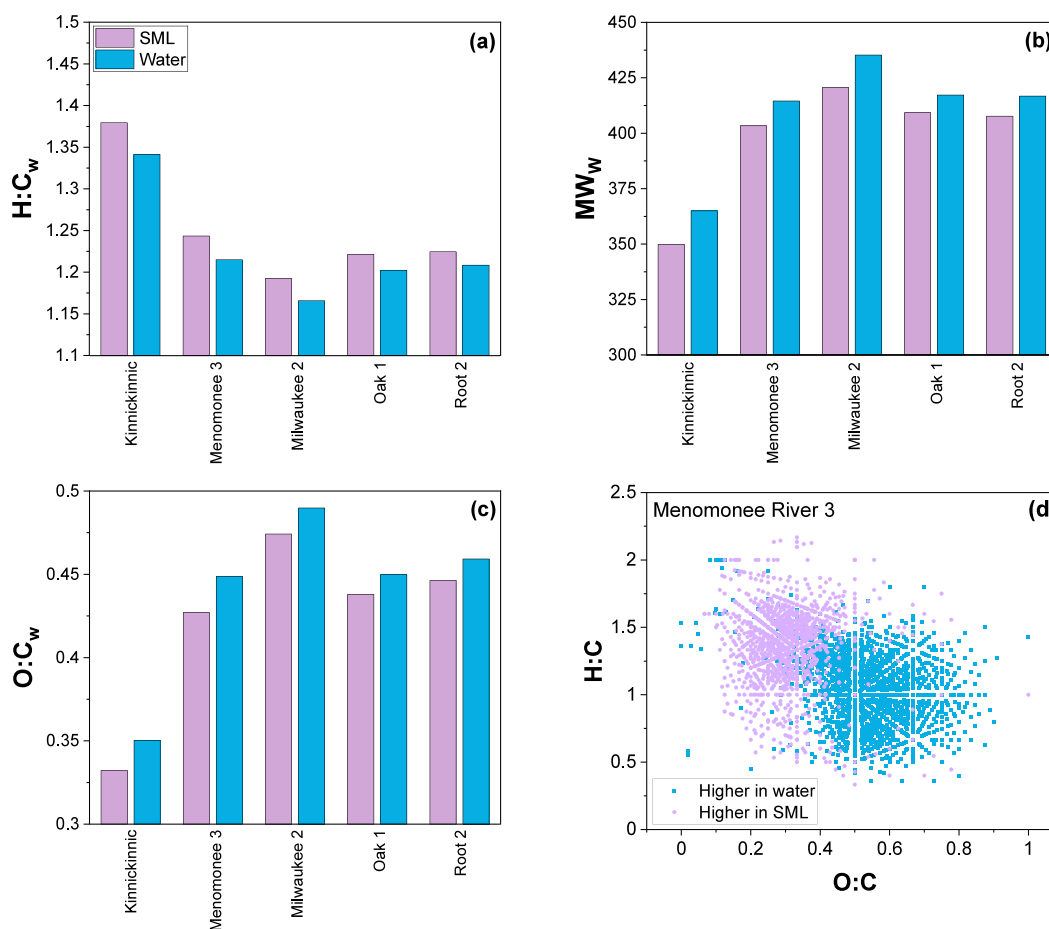


Figure 5. Weighted averages for (a) H:C, (b) molecular weight, and (c) O:C determined via FT-ICR MS for the surface microlayer (SML) and bulk water for the five major tributaries in Milwaukee. (d) Common DOM formulas that are at higher relative abundance in the SML (purple) and in the bulk water (blue) for Menomonee River 3. Data from the other four tributaries are plotted in Figure S6.

have percentages of PFCAs, PFSAs, and linear isomers that are similar to those of paired SML samples (Tables S27 and S28).

Sodium-normalized surface microlayer enrichment factors ($EF_{SML, norm}$) show that PFAS enrichment is limited under these conditions (Figure 2b, Tables S30 and S33). Average $EF_{SML, norm}$ values are 1.0–1.2 for PFCAs, with no trend with increasing chain length. Similar average $EF_{SML, norm}$ values of 0.9–1.2 are observed for short chain PFSAs, suggesting that there is minimal preferential partitioning of these PFAS to the SML. PFOS enrichment is observed in some samples, with $EF_{SML, norm}$ values ranging 0.7–5.2 (average = 1.4, $n = 26$). Similarly, $EF_{SML, norm}$ values of FOSA range 0.8–9.4 (average = 2.4, $n = 7$). While PFOS and FOSA are also enriched in natural foams (Figure 2a), it is noteworthy that there is no chain length-dependence in PFCAs in the SML. Collectively, $EF_{SML, norm}$ values indicate that longer chain PFOS and FOSA can partition to the SML, with high variability observed among different sites (i.e., a factor of 7.2 and 11.4 for PFOS and FOSA, respectively). Nonnormalized EF_{SML} values are not significantly different than $EF_{SML, norm}$ (Figure S12b, Table S34).

Reported EF_{SML} values for PFAS in previous studies range widely depending on sampling conditions, the sampling method, and water chemistry. Laboratory studies using marine seaspray (SML collection method: glass plate)³⁹ and synthetic water with varying salinity (metal screen)⁵⁹ report a wider range in EF_{SML} values (i.e., 1–85). As observed in natural foams, these studies report that SML enrichment increases with increasing chain

length for PFCAs and PFSAs, with preferential partitioning of PFSAs compared to PFCAs. For example, reported EF_{SML} in saline waters under laboratory conditions are 1–4 for PFOA and 10–85 for PFOS.^{39,59} In contrast, smaller EF_{SML} values are typically measured in marine field studies (e.g., <1 to 8 for PFSAs and PFCAs in Antarctica; glass plate),⁶⁰ with elevated values of 2–109 for PFOS in a nearshore coastal site in China (glass plate).³⁵ The average values reported here are lower than the average field-measured values of 1.5 for PFOA and 7.9 for PFOS in an AFFF-impacted lake, with similar values observed using two different glass-based sampling methods.⁶ Similar trends in preferential partitioning of long-chain PFAS are observed in air–water interfacial partitioning in unsaturated soils.^{34,43–45}

Water chemistry can potentially influence partitioning to the SML. For example, increased SML partitioning with increasing ionic strength^{36,47,48,59} is attributed to both increased hydrophobicity of the C–F chain³⁶ and decreased surface tension.⁴⁷ However, we observe a weak negative relationship between $\sum[\text{cations}]_{\text{water}}$ and $EF_{SML, PFOS}$ (Figure S15), which may be attributable to the small range in cation concentrations compared with previous studies. Interestingly, we also observe a weak negative trend between $EF_{SML, PFOS}$ and $[\text{DOC}]_{\text{water}}$. Previous studies report that DOM may either decrease PFAS partitioning to the SML via competition or increase PFAS partitioning by enhancing sorption of PFAS to DOM at the air–water interface.^{36,39,59} There is a weak positive correlation

between $EF_{SML,PFOS}$ and $[PFAS]_{water}$, as well as a negligible trend with pH_{water} . These results indicate that $[PFAS]_{water}$, rather than $[DOC]_{water}$, is a more important contributor to PFOS partitioning to the SML (Figure S15c,d). However, none of the $EF_{SML,PFOS}$ trends are statistically significant, which indicates that water chemistry plays a minor role in influencing SML partitioning under these conditions.

The low enrichment of PFAS to the SML compared to foams and compared to the air–water interface in unsaturated porous media is likely attributable to two factors. First, the specific surface area (i.e., ratio air–water interfacial area to bulk water volume) in surface waters is orders of magnitude lower than foams⁶ or in unsaturated porous media,^{41–43} which means that there is limited area to facilitate preferential partitioning. Second, it is likely that field conditions result in decreased partitioning to the SML compared to laboratory conditions. For example, tributary samples were collected from sites with flowing water, which results in mixing and may either limit the formation of the SML and/or prevent PFAS from reaching equilibrium. Similarly, most lake samples were collected during foaming events, which occur during highly turbulent conditions that facilitate air bubble formation.^{64,65} These well-mixed, turbulent conditions likely result in $EF_{SML, norm}$ values near 1 in many cases.

Preferential SML Partitioning of DOM. Dissolved organic carbon concentrations are 8.52 ± 3.80 mg of C/L in surface microlayer samples and 8.74 ± 3.51 mg of C/L in paired bulk water samples (Tables S6 and S7). These concentrations correspond to an average $EF_{SML, norm}$ of 1.00 ± 0.17 (Tables S30 and S33), which is lower than measurements in the Atlantic Ocean ($EF_{SML, norm} = 1.8 \pm 1.5$).⁵⁷ These values indicate that DOM is not preferentially enriched in the SML compared to bulk water under these conditions when it is assessed using bulk $[DOC]$ measurements.

However, high-resolution mass spectrometry demonstrates that there is preferential partitioning to the SML based on DOM composition. On average, there are 4840 formulas identified by FT-ICR MS in the five paired water and SML samples (Table S11). There are consistent differences in weighted averages derived from assigned formulas when comparing paired SML and water samples. For example, $H:C_w$ is consistently higher and DBE_w is consistently lower in SML samples (Figure 5 and Figure S5, Table S12), demonstrating that more aliphatic DOM preferentially partitions to the SML. This trend agrees with the observed decrease in the aromaticity of DOM in foam compared to the water column (Tables S5 and S6). Interestingly, the weighted average molecular weight (MW_w) is lower in SML samples compared to paired water samples, which is opposite the trend observed in $E_2:E_3$ in foam. However, it is important to note that FT-ICR MS is not a reliable measure of molecular weight.^{86,114} $O:C_w$ is lower in the SML in all cases, indicating that more reduced DOM preferentially partitions to the SML.

These trends are also observed in individual formulas present in the paired water and SML samples. Formulas with higher $H:C$ and lower $O:C$ values have higher relative abundance in the SML, suggesting that lipid- and peptide-like DOM¹¹⁵ preferentially partitions to the SML (Figure 5d and Figure S6). Conversely, formulas with higher relative abundance in the water column are more aromatic and oxidized, corresponding to more lignin- and tannin-like DOM.¹¹⁵ Collectively, the FT-ICR MS data demonstrate that DOM in the SML is more reduced, more aliphatic, and lower in apparent molecular weight than in bulk water.

Stronger correlations are observed between $EF_{SML, DOC}$ and water chemistry parameters compared to those of $EF_{SML, PFOS}$ (Figure S16). There are significant negative correlations between $EF_{SML, DOC}$ and $[DOC]_{water}$ and $[PFOS]_{water}$, as well as a weaker negative correlation with $[PFAS]_{water}$. These results may suggest inhibitive competition for enrichment at the SML between DOC and PFAS, although caution should be used when interpreting these relationships given the weak partitioning of DOC to the SML. There is also an unexpected weak negative trend between $EF_{SML, PFOS}$ and the sum of $[cations]_{water}$, as observed for $EF_{SML, PFOS}$.

Bulk DOM composition measurements indicate variable differences in the type of DOM in the SML compared to the underlying water column (Tables S5–S10). For example, DOM in the SML has higher apparent molecular weight (i.e., lower $E_2:E_3$)^{86,104} and is less aromatic (i.e., lower $SUVA_{254}$)^{104,105} than in bulk water in approximately half of the paired samples, as observed in the foam samples and as observed in $H:C_w$ in the SML by FT-ICR MS. However, opposite trends are observed in the remaining samples. Additionally, DOM in the SML is more microbial (i.e., higher fluorescence index),^{106–108} more algae-based (i.e., higher biological index),¹⁰⁶ and fresher (i.e., higher freshness index)¹⁰⁶ than corresponding bulk water in approximately half of the paired samples, with minor differences or opposite trends in the remaining samples. In all cases, differences in optical properties are small when comparing SML and bulk water samples (i.e., typically <5%). Thus, while we observe consistent preferential partitioning of DOM to the SML at the molecular level, bulk measurements of DOM concentration (i.e., $[DOC]$) and composition show only small differences. Overall, we conclude that partitioning of both PFAS and DOM to the SML in flowing and/or turbulent fresh surface waters is minor.

Environmental Implications. Understanding PFAS partitioning at the water surface in lakes and rivers is important for assessing exposure to wildlife and humans. The water surface (i.e., both SML and foam) can be enriched in organic carbon and serves as a food source for wildlife.^{64,67} We observed that PFAS concentrations in naturally formed foam are orders of magnitude higher than concentrations in bulk water, with normalized enrichment factors of 50–7500. Longer chain PFAS and PFSAs compared to PFCAs preferentially partition to foams. The enrichment of PFOS in the foam was correlated with increasing $[DOC]_{water}$, suggesting that DOM plays a role in facilitating PFOS accumulation. Dissolved organic carbon showed similar enrichment to foam as PFOA, with an average enrichment factor of 74. Interestingly, the DOM that preferentially partitions to foam is higher in apparent molecular weight than DOM in the water column, in agreement with the chain length trends observed for PFAS.

In contrast with natural foams, the enrichment of both PFAS and DOC in the surface microlayer is limited in the 28 studied surface waters. Although partitioning at the air–water interface plays a major role in PFAS transport in the subsurface,^{41–43,46–48} this finding is consistent with previous observations in a single lake⁶ and is likely attributable to the high surface area of foams compared to the SML. Furthermore, we hypothesize that flowing or turbulent systems (e.g., rivers or lakes on windy days) limit PFAS accumulation in the SML. Nevertheless, the individual PFAS that did show enrichment in the SML (i.e., PFOS and FOSA) also had the highest enrichment factors in foam. Although high-resolution mass spectrometry demonstrated preferential partitioning of aliphatic and reduced DOM to the SML, minor differences were observed

based on bulk measurements of DOM concentration and composition.

Collectively, this study demonstrates that naturally formed foam should be treated cautiously. We observed concentrations of >2300 ng/L in collapsed foam collected from water bodies with no known PFAS sources and with low bulk water concentrations, supporting recommendations from state agencies to avoid foams even in unimpacted waters.^{68,69} Despite the importance of air–water partitioning in the subsurface,^{41–43,46–48} this study indicates that SML partitioning in surface waters is minor.

■ ASSOCIATED CONTENT

SI Supporting Information

The Supporting Information is available free of charge at <https://pubs.acs.org/doi/10.1021/acs.est.4c02285>.

File 1 includes additional experimental detail; quality assurance measures; cation, DOC, and PFAS concentrations; pH, E₂:E₃, SUVA₂₅₄, and fluorescence indices for all samples; and FT-ICR MS data (PDF)

File 2 includes PFAS concentrations in all environmental samples (XLSX)

■ AUTHOR INFORMATION

Corresponding Author

Christina K. Remucal – Department of Civil and Environmental Engineering University of Wisconsin-Madison, Madison, Wisconsin 53706, United States; Environmental Chemistry and Technology Program University of Wisconsin-Madison, Madison, Wisconsin 53706, United States; Department of Chemistry University of Wisconsin-Madison, Madison, Wisconsin 53706, United States; orcid.org/0000-0003-4285-7638; Phone: (608) 262-1820; Email: remucal@wisc.edu

Authors

Summer L. Sherman-Bertinetti – Department of Civil and Environmental Engineering University of Wisconsin-Madison, Madison, Wisconsin 53706, United States

Edward G. Kostelnik – Environmental Chemistry and Technology Program University of Wisconsin-Madison, Madison, Wisconsin 53706, United States

Kaitlyn J. Gruber – Department of Chemistry University of Wisconsin-Madison, Madison, Wisconsin 53706, United States

Sarah Balgooyen – Department of Civil and Environmental Engineering University of Wisconsin-Madison, Madison, Wisconsin 53706, United States; orcid.org/0000-0003-3474-9602

Complete contact information is available at: <https://pubs.acs.org/10.1021/acs.est.4c02285>

Notes

The authors declare no competing financial interest.

■ ACKNOWLEDGMENTS

The authors thank Jenna Swenson, Thomas Pearson, and Samuel Bieber for assistance with sample collection, Sydney Van Frost for map preparation, James Lazarcik for maintaining instrumentation, Wisconsin Department of Natural Resources and many people, groups, and coalitions in Wisconsin for reporting foam sightings, and Martin Shafer for helpful discussions. Funding was provided by Wisconsin Sea Grant

(R/HCE-47) and a National Science Foundation Graduate Research Fellowship (K.J.G.).

■ REFERENCES

- (1) Anderko, L.; Pennea, E. Exposures to per- and polyfluoroalkyl substances (PFAS): Potential risks to reproductive and children's health. *Curr. Probl. Pediatr. Adolesc. Health Care* **2020**, *50* (2), No. 100760.
- (2) Schellenberger, S.; Liagkouridis, I.; Awad, R.; Khan, S.; Plassmann, M.; Peters, G.; Benskin, J. P.; Cousins, I. T. An outdoor aging study to investigate the release of per- and polyfluoroalkyl substances (PFAS) from functional textiles. *Environ. Sci. Technol.* **2022**, *56* (6), 3471–3479.
- (3) Johnson, A.; Shelton-Davenport, M.; Mantus, E. *Understanding, Controlling, and Preventing Exposure to PFAS: Proceedings of a Workshop—in Brief*. National Academies of Sciences, Engineering, and Medicine; Division on Earth and Life Studies; Environmental Health Matters Initiative; National Academies Press (US), 2020; p 12.
- (4) Gremmel, C.; Fromel, T.; Knepper, T. P. Systematic determination of perfluoroalkyl and polyfluoroalkyl substances (PFASs) in outdoor jackets. *Chemosphere* **2016**, *160*, 173–180.
- (5) Lanza, H. A.; Cochran, R. S.; Mudge, J. F.; Olson, A. D.; Blackwell, B. R.; Maul, J. D.; Salice, C. J.; Anderson, T. A. Temporal monitoring of perfluorooctane sulfonate accumulation in aquatic biota downstream of historical aqueous film forming foam use areas. *Environ. Toxicol. Chem.* **2017**, *36* (8), 2022–2029.
- (6) Schwichtenberg, T.; Bogdan, D.; Schaefer, C. E.; Stults, J.; Field, J. A. Per- and polyfluoroalkyl substances enrichment in the surface microlayer of a freshwater system impacted by aqueous film-forming foams. *ACS ES&T Water* **2023**, *3* (4), 1150–1160.
- (7) Schwichtenberg, T.; Bogdan, D.; Carignan, C. C.; Reardon, P.; Rewerts, J.; Wanzek, T.; Field, J. A. PFAS and dissolved organic carbon enrichment in surface water foams on a northern U.S. freshwater lake. *Environ. Sci. Technol.* **2020**, *54* (22), 14455–14464.
- (8) Reinikainen, J.; Perkola, N.; Aysto, L.; Sorvari, J. The occurrence, distribution, and risks of PFAS at AFFF-impacted sites in Finland. *Sci. Total Environ.* **2022**, *829*, No. 154237.
- (9) Hoisaeter, A.; Pfaff, A.; Breedveld, G. D. Leaching and transport of PFAS from aqueous film-forming foam (AFFF) in the unsaturated soil at a firefighting training facility under cold climatic conditions. *J. Contam. Hydrol.* **2019**, *222*, 112–122.
- (10) Baker, E. S.; Knappe, D. R. U. Per- and polyfluoroalkyl substances (PFAS)-contaminants of emerging concern. *Anal. Bioanal. Chem.* **2022**, *414* (3), 1187–1188.
- (11) Cousins, I. T.; DeWitt, J. C.; Gluge, J.; Goldenman, G.; Herzke, D.; Lohmann, R.; Ng, C. A.; Scheringer, M.; Wang, Z. The high persistence of PFAS is sufficient for their management as a chemical class. *Environ. Sci. Processes Impacts* **2020**, *22* (12), 2307–2312.
- (12) Saez, M.; de Voogt, P.; Parsons, J. R. Persistence of perfluoroalkylated substances in closed bottle tests with municipal sewage sludge. *Environ. Sci. Pollut. Res. Int.* **2008**, *15* (6), 472–477.
- (13) Brunn, H.; Arnold, G.; Körner, W.; Rippen, G.; Steinhäuser, K. G.; Valentin, I. PFAS: forever chemicals—Persistent, bioaccumulative and mobile. Reviewing the status and the need for their phase out and remediation of contaminated sites. *Environ. Sci. Eur.* **2023**, *35* (1), 20.
- (14) Lesmeister, L.; Lange, F. T.; Breuer, J.; Biegel-Engler, A.; Giese, E.; Scheurer, M. Extending the knowledge about PFAS bioaccumulation factors for agricultural plants - A review. *Sci. Total Environ.* **2021**, *766*, No. 142640.
- (15) George, S. E.; Baker, T. R.; Baker, B. B. Nonlethal detection of PFAS bioaccumulation and biomagnification within fishes in an urban- and wastewater-dominant Great Lakes watershed. *Environ. Pollut.* **2023**, *321*, No. 121123.
- (16) Remucal, C. K. Spatial and temporal variability of perfluoroalkyl substances in the Laurentian Great Lakes. *Environ. Sci. Processes Impacts* **2019**, *21* (11), 1816–1834.
- (17) Burkhard, L. P. Evaluation of published bioconcentration factor (BCF) and bioaccumulation factor (BAF) data for per- and polyfluoroalkyl substances across aquatic species. *Environ. Toxicol. Chem.* **2021**, *40* (6), 1530–1543.

- (18) Ren, J.; Point, A. D.; Baygi, S. F.; Fernando, S.; Hopke, P. K.; Holsen, T. M.; Crimmins, B. S. Bioaccumulation of polyfluoroalkyl substances in the Lake Huron aquatic food web. *Sci. Total Environ.* **2022**, *819*, No. 152974.
- (19) Haukas, M.; Berger, U.; Hop, H.; Gulliksen, B.; Gabrielsen, G. W. Bioaccumulation of per- and polyfluorinated alkyl substances (PFAS) in selected species from the Barents Sea food web. *Environ. Pollut.* **2007**, *148* (1), 360–371.
- (20) Saikat, S.; Kreis, I.; Davies, B.; Bridgman, S.; Kamanyire, R. The impact of PFOS on health in the general population: a review. *Environ. Sci.: Processes Impacts* **2013**, *15* (2), 329–335.
- (21) Cui, L.; Zhou, Q. F.; Liao, C. Y.; Fu, J. J.; Jiang, G. B. Studies on the toxicological effects of PFOA and PFOS on rats using histological observation and chemical analysis. *Arch. Environ. Contam. Toxicol.* **2009**, *56* (2), 338–349.
- (22) Tarapore, P.; Ouyang, B. Perfluoroalkyl chemicals and male reproductive health: Do PFOA and PFOS increase risk for male infertility? *Int. J. Environ. Res. Public Health* **2021**, *18* (7), 3794.
- (23) Betts, K. PFOS and PFOA in humans: New study links prenatal exposure to lower birth weight. *Environ. Health Perspect.* **2007**, *115* (11), A550.
- (24) Jane, L. E. L.; Yamada, M.; Ford, J.; Owens, G.; Prow, T.; Juhasz, A. Health-related toxicity of emerging per- and polyfluoroalkyl substances: Comparison to legacy PFOS and PFOA. *Environ. Res.* **2022**, *212* (Pt C), No. 113431.
- (25) Pfothenauer, D.; Sellers, E.; Olson, M.; Praedel, K.; Shafer, M. PFAS concentrations and deposition in precipitation: An intensive 5-month study at National Atmospheric Deposition Program – National trends sites (NADP-NTN) across Wisconsin. *USA. Atmos. Environ.* **2022**, *291*, No. 119368.
- (26) Cousins, I. T.; Johansson, J. H.; Salter, M. E.; Sha, B.; Scheringer, M. Outside the safe operating space of a new planetary boundary for per- and polyfluoroalkyl substances (PFAS). *Environ. Sci. Technol.* **2022**, *56* (16), 11172–11179.
- (27) Kim, Y.; Pike, K. A.; Gray, R.; Sprinkle, J. W.; Faust, J. A.; Edmiston, P. L. Non-targeted identification and semi-quantitation of emerging per- and polyfluoroalkyl substances (PFAS) in US rainwater. *Environ. Sci. Processes Impacts* **2023**, *25*, 1771–1787.
- (28) Giesy, J. P.; Mabury, S. A.; Martin, J. W.; Kannan, K.; Jones, P. D.; Newsted, J. L.; Coady, K. Perfluorinated compounds in the Great Lakes. In: *The Handbook of Environmental Chemistry* **2006**, *5N*, 391–438.
- (29) Lin, Y.; Capozzi, S. L.; Lin, L.; Rodenburg, L. A. Source apportionment of perfluoroalkyl substances in Great Lakes fish. *Environ. Pollut.* **2021**, *290*, No. 118047.
- (30) Codling, G.; Sturchio, N. C.; Rockne, K. J.; Li, A.; Peng, H.; Tse, T. J.; Jones, P. D.; Giesy, J. P. Spatial and temporal trends in poly- and perfluorinated compounds in the Laurentian Great Lakes Erie, Ontario, and St. Clair. *Environ. Pollut.* **2018**, *237*, 396–405.
- (31) Pickard, H. M.; Crisciottiello, A. S.; Persaud, D.; Spencer, C.; Muir, D. C. G.; Lehnher, I.; Sharp, M. J.; De Silva, A. O.; Young, C. J. Ice core record of persistent short-chain fluorinated alkyl acids: Evidence of the impact from global environmental regulations. *Geophys. Res. Lett.* **2020**, *47* (10), No. e2020GL087535.
- (32) MacInnis, J.; De Silva, A. O.; Lehnher, I.; Muir, D. C. G.; St Pierre, K. A.; St Louis, V. L.; Spencer, C. Investigation of perfluoroalkyl substances in proglacial rivers and permafrost seep in a high Arctic watershed. *Environ. Sci.: Processes Impacts* **2022**, *24* (1), 42–51.
- (33) Muir, D.; Bossi, R.; Carlsson, P.; Evans, M.; De Silva, A.; Halsall, C.; Rauer, C.; Herzke, D.; Hung, H.; Letcher, R.; Rigét, F.; Roos, A. Levels and trends of poly- and perfluoroalkyl substances in the Arctic environment – An update. *Emerg. Contam.* **2019**, *5*, 240–271.
- (34) Guo, B.; Saleem, H.; Brusseau, M. L. Predicting interfacial tension and adsorption at fluid-fluid interfaces for mixtures of PFAS and/or hydrocarbon surfactants. *Environ. Sci. Technol.* **2023**, *57* (21), 8044–8052.
- (35) Ju, X.; Jin, Y.; Sasaki, K.; Saito, N. Perfluorinated surfactants in surface, subsurface water and microlayer from Dalian Coastal waters in China. *Environ. Sci. Technol.* **2008**, *42* (10), 3538–3542.
- (36) McMurdo, C. J.; Ellis, D. A.; Webster, E.; Butler, J.; Christensen, R. D.; Reid, L. K. Aerosol enrichment of the surfactant PFO and mediation of the water–air transport of gaseous PFOA. *Environ. Sci. Technol.* **2008**, *42* (11), 3969–3974.
- (37) Brusseau, M. L.; Van Glubt, S. The influence of surfactant and solution composition on PFAS adsorption at fluid-fluid interfaces. *Water Res.* **2019**, *161*, 17–26.
- (38) Wang, S.; Wang, H.; Zhao, W.; Cao, Y.; Wan, Y. Investigation on the distribution and fate of perfluorooctane sulfonate (PFOS) and perfluorooctanoate (PFOA) in a sewage-impacted bay. *Environ. Pollut.* **2015**, *205*, 186–198.
- (39) Johansson, J. H.; Salter, M. E.; Acosta Navarro, J. C.; Leck, C.; Nilsson, E. D.; Cousins, I. T. Global transport of perfluoroalkyl acids via sea spray aerosol. *Environ. Sci. Processes Impacts* **2019**, *21* (4), 635–649.
- (40) Reth, M.; Berger, U.; Broman, D.; Cousins, I. T.; Nilsson, E. D.; McLachlan, M. S. Water-to-air transfer of perfluorinated carboxylates and sulfonates in a sea spray simulator. *Environ. Chem.* **2011**, *8* (4), 381.
- (41) Chen, S.; Guo, B. Pore-scale modeling of PFAS transport in water-unsaturated porous media: Air–water interfacial adsorption and mass-transfer processes in thin water films. *Water Resour. Res.* **2023**, *59* (8), No. e2023WR034664.
- (42) Guo, B.; Zeng, J.; Brusseau, M. L. A Mathematical model for the release, transport, and retention of per- and polyfluoroalkyl substances (PFAS) in the vadose zone. *Water Resour. Res.* **2020**, *56* (2), No. e2019WR026667.
- (43) Brusseau, M. L.; Guo, B. PFAS concentrations in soil versus soil porewater: Mass distributions and the impact of adsorption at air-water interfaces. *Chemosphere* **2022**, *302*, No. 134938.
- (44) Lyu, Y.; Wang, B.; Du, X.; Guo, B.; Brusseau, M. L. Air-water interfacial adsorption of C₄-C₁₀ perfluorocarboxylic acids during transport in unsaturated porous media. *Sci. Total Environ.* **2022**, *831*, No. 154905.
- (45) Stults, J. F.; Choi, Y. J.; Rockwell, C.; Schaefer, C. E.; Nguyen, D. D.; Knappe, D. R. U.; Illangasekare, T. H.; Higgins, C. P. Predicting concentration- and ionic-strength-dependent air-water interfacial partitioning parameters of PFASs using quantitative structure-property relationships (QSPPRs). *Environ. Sci. Technol.* **2023**, *57* (13), 5203–5215.
- (46) Brusseau, M. L. Assessing the potential contributions of additional retention processes to PFAS retardation in the subsurface. *Sci. Total Environ.* **2018**, *613–614*, 176–185.
- (47) Costanza, J.; Arshadi, M.; Abriola, L. M.; Pennell, K. D. Accumulation of PFOA and PFOS at the air–water interface. *Environ. Sci. Technol. Lett.* **2019**, *6* (8), 487–491.
- (48) Schaefer, C. E.; Culina, V.; Nguyen, D.; Field, J. Uptake of poly- and perfluoroalkyl substances at the air-water interface. *Environ. Sci. Technol.* **2019**, *53* (21), 12442–12448.
- (49) Yuan, S.; Wang, X.; Jiang, Z.; Zhang, H.; Yuan, S. Contribution of air-water interface in removing PFAS from drinking water: Adsorption, stability, interaction and machine learning studies. *Water Res.* **2023**, *236*, No. 119947.
- (50) Meng, P.; Deng, S.; Lu, X.; Du, Z.; Wang, B.; Huang, J.; Wang, Y.; Yu, G.; Xing, B. Role of air bubbles overlooked in the adsorption of perfluorooctanesulfonate on hydrophobic carbonaceous adsorbents. *Environ. Sci. Technol.* **2014**, *48* (23), 13785–13792.
- (51) Meng, P.; Jiang, X.; Wang, B.; Huang, J.; Wang, Y.; Yu, G.; Cousins, I. T.; Deng, S. Role of the air-water interface in removing perfluoroalkyl acids from drinking water by activated carbon treatment. *J. Hazard Mater.* **2020**, *386*, No. 121981.
- (52) Cunliffe, M.; Engel, A.; Frka, S.; Gašparović, B.; Guitart, C.; Murrell, J. C.; Salter, M.; Stolle, C.; Upstill-Goddard, R.; Wurl, O. Sea surface microlayers: A unified physicochemical and biological perspective of the air–ocean interface. *Prog. Oceanogr.* **2013**, *109*, 104–116.
- (53) Engel, A.; Sperling, M.; Sun, C.; Grosse, J.; Friedrichs, G. Organic matter in the surface microlayer: Insights from a wind wave channel experiment. *Front. Mar. Sci.* **2018**, *5*, 182.
- (54) Huang, Y. J.; Brimblecombe, P.; Lee, C. L.; Latif, M. T. Surfactants in the sea-surface microlayer and sub-surface water at

- estuarine locations: Their concentration, distribution, enrichment, and relation to physicochemical characteristics. *Mar. Pollut. Bull.* **2015**, *97* (1–2), 78–84.
- (55) Elzerman, A. W.; Armstrong, D. E. Enrichment of Zn, Cd, Pb, and Cu in the surface microlayer of Lakes Michigan, Ontario, and Mendota. *Limnol. Oceanogr.* **1979**, *24* (1), 133–144.
- (56) Jayarathne, T.; Gamage, D. K.; Prather, K. A.; Stone, E. A.; Croot, P. Enrichment of saccharides at the air–water interface: A quantitative comparison of sea surface microlayer and foam. *Environ. Chem.* **2023**, *19* (8), 506–516.
- (57) van Pinxteren, M.; Barthel, S.; Fomba, K. W.; Müller, K.; von Tümpling, W.; Herrmann, H.; Deming, J. W.; Thomsen, L. The influence of environmental drivers on the enrichment of organic carbon in the sea surface microlayer and in submicron aerosol particles – measurements from the Atlantic Ocean. *Elementa: Sci. Anthropocene* **2017**, *5*, 35.
- (58) Ritchie, K. B.; Smith, G. W. Microbial communities of coral surface mucopolysaccharide layers. In: Rosenberg, E.; Loya, Y. (eds) *Coral Health and Disease*. Springer: Berlin, Heidelberg, 2004, 259–264.
- (59) Schaefer, C. E.; Lemes, M. C. S.; Schwichtenberg, T.; Field, J. A. Enrichment of poly- and perfluoroalkyl substances (PFAS) in the surface microlayer and foam in synthetic and natural waters. *J. Hazard. Mater.* **2022**, *440*, No. 129782.
- (60) Casas, G.; Martinez-Varela, A.; Roscales, J. L.; Vila-Costa, M.; Dachs, J.; Jimenez, B. Enrichment of perfluoroalkyl substances in the sea-surface microlayer and sea-spray aerosols in the Southern Ocean. *Environ. Pollut.* **2020**, *267*, No. 115512.
- (61) Schaefer, C. E.; Nguyen, D.; Meng, P.; Fang, Y.; Knappe, D. R. U. Sorption of perfluoroalkyl ether carboxylic acids (PFECAs) at the air-water interface in porous media: Modeling perspectives. *J. Hazard. Mater. Adv.* **2022**, *6*, No. 100062.
- (62) Li, Z.; Lyu, X.; Gao, B.; Xu, H.; Wu, J.; Sun, Y. Effects of ionic strength and cation type on the transport of perfluorooctanoic acid (PFOA) in unsaturated sand porous media. *J. Hazard. Mater.* **2021**, *403*, No. 123688.
- (63) Lyu, Y.; Brusseau, M. L. The influence of solution chemistry on air-water interfacial adsorption and transport of PFOA in unsaturated porous media. *Sci. Total Environ.* **2020**, *713*, No. 136744.
- (64) Schilling, K.; Zessner, M. Foam in the aquatic environment. *Water Res.* **2011**, *45* (15), 4355–4366.
- (65) Stefani, F.; Salerno, F.; Copetti, D.; Rabuffetti, D.; Guidetti, L.; Torri, G.; Naggi, A.; Iacomini, M.; Morabito, G.; Guzzella, L. Endogenous origin of foams in lakes: A long-term analysis for Lake Maggiore (northern Italy). *Hydrobiologia* **2016**, *767* (1), 249–265.
- (66) Wegner, C.; Hamburger, M. Occurrence of stable foam in the upper Rhine River caused by plant-derived surfactants. *Environ. Sci. Technol.* **2002**, *36* (15), 3250–3256.
- (67) Napolitano, G. E.; Richmond, J. E. Enrichment of biogenic lipids, hydrocarbons and PCBs in stream-surface foams. *Environ. Toxicol. Chem.* **1995**, *14* (2), 197–201.
- (68) DNR confirms PFAS-containing foam found in Peshtigo area waterways. Wisconsin Department of Natural Resources **2019**. <https://dnr.wi.gov/news/releases/article/?id=4932>.
- (69) PFAS foam on lakes and streams. Michigan Department of Environment, Great Lakes, and Energy **2021**. <https://www.michigan.gov/pfasresponse/investigations/lakes-and-streams/foam>.
- (70) PFAS in sea foam along Dutch coast. *National Institute for Public Health and the Environment, RIVM* **2023**. <https://www.rivm.nl/en/news/pfas-in-sea-foam-along-dutch-coast>.
- (71) Boztas, S. Netherlands warns children not to swallow sea foam over PFAS concerns. *Guardian* **2023**. <https://www.theguardian.com/environment/2023/dec/13/netherlands-children-not-swallow-sea-foam-pfas-concerns>.
- (72) Burns, D. J.; Stevenson, P.; Murphy, P. J. C. PFAS removal from groundwaters using surface-active foam fractionation. *Remediation* **2021**, *31* (4), 19–33.
- (73) Lee, Y.-C.; Wang, P.-Y.; Lo, S.-L.; Huang, C. P. Recovery of perfluorooctane sulfonate (PFOS) and perfluorooctanoate (PFOA) from dilute water solution by foam flotation. *Sep. Purif. Technol.* **2017**, *173*, 280–285.
- (74) McCleaf, P.; Kjellgren, Y.; Ahrens, L. Foam fractionation removal of multiple per- and polyfluoroalkyl substances from landfill leachate. *AWWA Water Sci.* **2021**, *3* (5), No. e1238.
- (75) Meng, P.; Deng, S.; Maimaiti, A.; Wang, B.; Huang, J.; Wang, Y.; Cousins, I. T.; Yu, G. Efficient removal of perfluorooctane sulfonate from aqueous film-forming foam solution by aeration-foam collection. *Chemosphere* **2018**, *203*, 263–270.
- (76) Simmler, W. Adsorptive bubble separation techniques. Herausgeg. v.R. Lemlich. Academic Press, New York-London 1972. 1. Aufl., 331 S., 104 Abb. *Chemie Ingenieur Technik - CIT* **1973**, *45* (4), 228–228.
- (77) Smith, S. J.; Wiberg, K.; McCleaf, P.; Ahrens, L. Pilot-scale continuous foam fractionation for the removal of per- and polyfluoroalkyl substances (PFAS) from landfill leachate. *ACS ES&T Water* **2022**, *2* (5), 841–851.
- (78) *Surface water PFAS sampling*. Michigan Department of Environment, Great Lakes, and Energy. <https://www.michigan.gov/-/media/Project/Websites/PFAS-Response/Sampling-Guidance/Surface-Water.pdf?rev=a4a35607c5ba4a5c83de17928c693aec>.
- (79) Harvey, G. W. Microlayer collection from the sea surface: A new method and initial results. *Limnol. Oceanogr.* **1966**, *11* (4), 608–613.
- (80) U.S. Environmental Protection Agency Draft Method 1633: *Analysis of per- and polyfluoroalkyl substances (PFAS) in aqueous, solid, biosolids, and tissue samples by LC-MS/MS (EPA 821-D-21-001)*. 2021.
- (81) Dittmar, T.; Koch, B.; Hertkorn, N.; Kattner, G. A simple and efficient method for the solid-phase extraction of dissolved organic matter (SPE-DOM) from seawater. *Limnol. Oceanogr. Meth.* **2008**, *6* (6), 230–235.
- (82) Ziegler, G.; Gonsior, M.; Fisher, D. J.; Schmitt-Kopplin, P.; Tamburri, M. N. Formation of brominated organic compounds and molecular transformations in dissolved organic matter (DOM) after ballast water treatment with sodium dichloroisocyanurate dihydrate (DICD). *Environ. Sci. Technol.* **2019**, *53* (14), 8006–8016.
- (83) Milstead, R. P.; Remucal, C. K. Molecular-level insights into the formation of traditional and novel halogenated disinfection byproducts. *ACS ES&T Water* **2021**, *1* (8), 1966–1974.
- (84) Berg, S. M.; Whiting, Q. T.; Herli, J. A.; Winkels, R.; Wammer, K. H.; Remucal, C. K. The role of dissolved organic matter composition in determining photochemical reactivity at the molecular level. *Environ. Sci. Technol.* **2019**, *53* (20), 11725–11734.
- (85) Maizel, A. C.; Li, J.; Remucal, C. K. Relationships between dissolved organic matter composition and photochemistry in lakes of diverse trophic status. *Environ. Sci. Technol.* **2017**, *51* (17), 9624–9632.
- (86) Maizel, A. C.; Remucal, C. K. Molecular composition and photochemical reactivity of size-fractionated dissolved organic matter. *Environ. Sci. Technol.* **2017**, *51* (4), 2113–2123.
- (87) Maizel, A. C.; Remucal, C. K. The effect of advanced secondary municipal wastewater treatment on the molecular composition of dissolved organic matter. *Water Res.* **2017**, *122*, 42–52.
- (88) Koch, B. P.; Dittmar, T.; Witt, M.; Kattner, G. Fundamentals of molecular formula assignment to ultrahigh resolution mass data of natural organic matter. *Anal. Chem.* **2007**, *79* (4), 1758–1763.
- (89) Wasserman, I. 'Something has to be done': Living along Madison's Starkweather Creek, one of Wisconsin's most polluted waterways. *Wisconsin Public Radio* 2021. <https://www.wpr.org/something-has-be-done-living-along-madisons-starkweather-creek-one-wisconsins-most-polluted>.
- (90) PFAS contamination in the City of Madison and Dane County. *Wisconsin Department of Natural Resources*. <https://dnr.wisconsin.gov/topic/PFAS/DaneCounty.html>.
- (91) Stocks, A.; Haag, C. DNR releases latest sampling results revealing broader PFAS presence in Madison area lakes and Yahara river chain. *Wisconsin Department of Natural Resources* 2021 <https://dnr.wisconsin.gov/newsroom/release/40561>.

- (92) PFAS contamination in the Marinette and Peshtigo area. *Wisconsin Department of Natural Resources* <https://dnr.wisconsin.gov/topic/PFAS/Marinette.html>.
- (93) Balgooyen, S.; Remucal, C. K. Impacts of environmental and engineered processes on the PFAS fingerprint of fluorotelomer-based AFFF. *Environ. Sci. Technol.* **2023**, *57* (1), 244–254.
- (94) We, A. C. E.; Stickland, A. D.; Clarke, B. O.; Freguia, S. The role of suspended biomass in PFAS enrichment in wastewater treatment foams. *Water Res.* **2024**, *254*, No. 121349.
- (95) Mussabek, D.; Ahrens, L.; Persson, K. M.; Berndtsson, R. Temporal trends and sediment-water partitioning of per- and polyfluoroalkyl substances (PFAS) in lake sediment. *Chemosphere* **2019**, *227*, 624–629.
- (96) Balgooyen, S.; Remucal, C. K. Tributary loading and sediment desorption as sources of PFAS to receiving waters. *ACS ES&T Water* **2022**, *2* (3), 436–445.
- (97) Munoz, G.; Budzinski, H.; Babut, M.; Lobry, J.; Selleslagh, J.; Tapie, N.; Labadie, P. Temporal variations of perfluoroalkyl substances partitioning between surface water, suspended sediment, and biota in a macrotidal estuary. *Chemosphere* **2019**, *233*, 319–326.
- (98) Labadie, P.; Chevreuil, M. Partitioning behaviour of perfluorinated alkyl contaminants between water, sediment and fish in the Orge River (nearby Paris, France). *Environ. Pollut.* **2011**, *159* (2), 391–397.
- (99) Goodrow, S. M.; Ruppel, B.; Lippincott, R. L.; Post, G. B.; Procopio, N. A. Investigation of levels of perfluoroalkyl substances in surface water, sediment and fish tissue in New Jersey, USA. *Sci. Total Environ.* **2020**, *729*, No. 138839.
- (100) de Wit, C. A.; Bossi, R.; Dietz, R.; Dreyer, A.; Faxneld, S.; Garbus, S. E.; Hellstrom, P.; Koschorreck, J.; Lohmann, N.; Roos, A.; Sellstrom, U.; Sonne, C.; Treu, G.; Vorkamp, K.; Yuan, B.; Eulaers, I. Organohalogen compounds of emerging concern in Baltic Sea biota: Levels, biomagnification potential and comparisons with legacy contaminants. *Environ. Int.* **2020**, *144*, No. 106037.
- (101) Conder, J. M.; Hoke, R. A.; De Wolf, W.; Russell, M. H.; Buck, R. C. Are PFCAs bioaccumulative? A critical review and comparison with regulatory criteria and persistent lipophilic compounds. *Environ. Sci. Technol.* **2008**, *42* (4), 995–1003.
- (102) Martin, J. W.; Mabury, S. A.; Solomon, K. R.; Muir, D. C. G. Bioconcentration and tissue distribution of perfluorinated acids in rainbow trout (*Oncorhynchus mykiss*). *Environ. Toxicol. Chem.* **2003**, *22* (1), 196–204.
- (103) Dai, X.; Xie, Z.; Dorian, B.; Gray, S.; Zhang, J. Comparative study of PFAS treatment by UV, UV/ozone, and fractionations with air and ozonated air. *Environ. Sci. Water Res. Technol.* **2019**, *5* (11), 1897–1907.
- (104) Helms, J. R.; Stubbins, A.; Ritchie, J. D.; Minor, E. C.; Kieber, D. J.; Mopper, K. Absorption spectral slopes and slope ratios as indicators of molecular weight, source, and photobleaching of chromophoric dissolved organic matter. *Limnol. Oceanogr.* **2008**, *53* (3), 955–969.
- (105) Weishaar, J. L.; Aiken, G. R.; Bergamaschi, B. A.; Fram, M. S.; Fujii, R.; Mopper, K. Evaluation of specific ultraviolet absorbance as an indicator of the chemical composition and reactivity of dissolved organic carbon. *Environ. Sci. Technol.* **2003**, *37* (20), 4702–4708.
- (106) Hansen, A. M.; Kraus, T. E. C.; Pellerin, B. A.; Fleck, J. A.; Downing, B. D.; Bergamaschi, B. A. Optical properties of dissolved organic matter (DOM): Effects of biological and photolytic degradation. *Limnol. Oceanogr.* **2016**, *61* (3), 1015–1032.
- (107) Minor, E. C.; Swenson, M. M.; Mattson, B. M.; Oyler, A. R. Structural characterization of dissolved organic matter: a review of current techniques for isolation and analysis. *Environ. Sci. Processes Impacts* **2014**, *16* (9), 2064–2079.
- (108) Peterson, B. M.; McNally, A. M.; Cory, R. M.; Thoemke, J. D.; Cotner, J. B.; McNeill, K. Spatial and temporal distribution of singlet oxygen in Lake Superior. *Environ. Sci. Technol.* **2012**, *46* (13), 7222–7229.
- (109) McKnight, D. M.; Boyer, E. W.; Westerhoff, P. K.; Doran, P. T.; Kulbe, T.; Andersen, D. T. Spectrofluorometric characterization of dissolved organic matter for indication of precursor material and aromaticity. *Limnol. Oceanogr.* **2001**, *46* (1), 38–48.
- (110) Ohno, T. Fluorescence inner-filtering correction for determining the humification index of dissolved organic matter. *Environ. Sci. Technol.* **2002**, *36* (4), 742–746.
- (111) Zsolnay, A.; Baigar, E.; Jimenez, M.; Steinweg, B.; Saccomandi, F. Differentiating with fluorescence spectroscopy the sources of dissolved organic matter in soils subjected to drying. *Chemosphere* **1999**, *38* (1), 45–50.
- (112) Forever Chemicals in Our Water. *Milwaukee Riverkeeper* <https://milwaukeekeeper.org/pfas/>.
- (113) Bergquist, L. DNR orders Mitchell Airport to cleanup ‘forever’ chemicals detected in Lake Michigan tributaries. *Milwaukee J. Sentinel* **2019** <https://www.jsonline.com/story/news/local/milwaukee/2019/10/18/stormwater-mitchell-airport-contains-forever-chemicals/4023687002/>.
- (114) Remucal, C. K.; Cory, R. M.; Sander, M.; McNeill, K. Low molecular weight components in an aquatic humic substance as characterized by membrane dialysis and Orbitrap mass spectrometry. *Environ. Sci. Technol.* **2012**, *46* (17), 9350–9359.
- (115) Laszakovits, J. R.; MacKay, A. A. Data-based chemical class regions for van Krevelen diagrams. *J. Am. Soc. Mass Spectrom.* **2022**, *33* (1), 198–202.